Apoptosis or senescence-like growth arrest: influence of cell-cycle position, p53, p21 and bax in H_2O_2 response of normal human fibroblasts

Qin M. CHEN[1], Juping LIU and Jessica B. MERRETT

Department of Pharmacology, Skaggs Pharmaceutical Sciences Building, Room 130, University of Arizona, 1703 E. Mabel Street, Tucson, AZ 85721, U.S.A.

Early-passage human diploid fibroblasts (HDFs) undergo senescence-like growth arrest in response to sublethal concentrations of H_2O_2 [Chen and Ames (1994) Proc. Natl. Acad. Sci. U.S.A. **95**, 4130–4134]. We determine here whether H_2O_2 can cause apoptosis in HDFs and the molecular changes that differ between apoptosis and senescence-like growth arrest. When exponentially growing early-passage IMR-90 cells were treated for 2 h with 50–200 μM (or 0.25–1 pmol/cell) H_2O_2, a fraction of cells detached at 16–32 h after the treatment. The cells remaining attached were growth-arrested and developed features of senescence in 1 week. The detached cells showed caspase-3 activation and typical morphological changes associated with apoptosis. Caspase-3 activation was H_2O_2 dose-dependent and preceded nuclear condensation or plasma membrane leakage. Apoptotic cells were mainly distributed in the S-phase of the cell cycle, while growth-arrested cells exhibited predominantly G1- and G2/M-phase distributions. H_2O_2 pretreatment induced G1 arrest and prohibited induction of apoptosis by a subsequent H_2O_2 chal lenge. The p53 protein showed an average 6.1-fold elevation in apoptotic cells and a 3.5-fold elevation in growth-arrested cells. Reduction of p53 levels with human papillomavirus E6 protein prohibited the activation of caspase-3 and decreased the proportion of apoptotic cells. Growth-arrested cells had elevated p21, while p21 was absent in apoptotic cells. Bcl-2 was elevated in both growth-arrested and apoptotic cells. Finally, although the overall level of bax did not change in growth-arrested or apoptotic cells, the solubility of bax protein increased in apoptotic cells. Our data suggest that in contrast with growth-arrested cells, apoptotic cells show an S-phase cell cycle distribution, a higher degree of p53 elevation, an absence of p21 protein and increased solubility of bax protein.

Key words: caspases, G1 arrest, oxidants, S-phase

INTRODUCTION

Oxidants are ubiquitous. Mitochondrial respiration and oxidases produce oxidants as by-products [1–4]. In addition to these continuous sources, oxidants are generated by inflammatory responses, ischaemic reperfusion, smoking, certain environmental toxins and metabolism of xenobiotics [1–4]. As estimated, the steady-state H_2O_2 concentration in an animal liver is about 0.1 μM and can be higher in other areas where H_2O_2 detoxification is less efficient [5]. Although the scavenger enzymes superoxide dismutase, catalase and glutathione peroxidases can remove oxidants, the oxidants that escape from these enzymes can damage biomacromolecules, cells and organisms. The accumulated oxidative damage has been postulated as an important cause of aging, cancer and degenerative diseases [1,6].

How normal somatic cells inside our body deal with oxidative damage is not entirely clear. Unlike tumour cells or immortalized rodent cells, normal human cells maintain a normal karyotype and can only replicate a limited number of times under culture conditions [7–10]. Normal human diploid fibroblasts (HDFs) from fetal tissues can replicate 50–60 times in tissue culture, thus providing a stable system for identifying cellular and molecular changes produced by oxidants. At the end of their replicative life span, HDFs reach a stable state of senescence. Senescent cells are irreversibly growth-arrested and contain elevated levels of p21 and p16 cyclin-dependent kinase inhibitors [11,12]. A number of molecular changes found in senescent cells resemble those occurring in somatic cells during the process of aging *in vivo* [13].

We previously reported that early passage HDFs surviving H_2O_2 treatment undergo senescence-like growth arrest [14,15]. H_2O_2 induces transient elevation of p53 protein and sustained elevation of p21 protein [16]. These cells cannot hyperphosphorylate retinoblastoma protein but show a prolonged G1 arrest and resemble senescent cells morphologically [14,16]. Since oxidants have been reported to cause apoptosis in many experimental systems, we test here whether H_2O_2 causes apoptosis in HDFs and, if so, what critical molecular changes take place in apoptotic cells.

Apoptosis is a type of programmed cell death characterized by the morphological changes of nuclear condensation and cell shrinkage [17,18]. Many DNA-damaging agents can induce an elevation of p53 tumour suppressor protein and cause apoptosis in a p53-dependent manner [19]. Changes in p53 precede an imbalance of survival versus pro-apoptotic factors in the bcl-2 family [19–21]. Activation of caspases ultimately results in cell degradation [22,23]. Here we test whether changes in p53, bcl-2/bax and caspase-3 occur in apoptotic HDFs as a result of oxidative stress.

MATERIALS AND METHODS

Cell culture and treatment with H_2O_2

IMR-90 cells [obtained from the Coriell Institute for Medical Research (Camden, NJ, U.S.A.) at the population doubling level (PDL) of 10.9] were subcultured weekly in 10 ml of Dulbecco's modified Eagle's medium (DMEM) (Gibco BRL, Grand Island, NY, U.S.A.) with 10 % fetal bovine serum (FBS) (Gibco BRL) at a seeding density of 0.5×10^6 cells/100 mm diameter dish. Upon confluence, there were approx. $6–7 \times 10^6$ early-passage cells in

Abbreviations used: AMC, 7-amino-4-methylcoumarin; BrdU, bromodeoxyuridine; DMEM, Dulbecco's modified Eagle's medium; FBS, fetal bovine serum; HDFs, human diploid fibroblasts; HPV, human papilloma virus; PDL, population doubling level; Pdml, propidium iodide; SA β-gal, senescence-associated β-galactosidase.

[1] To whom correspondence should be addressed (e-mail chen@pharmacy.arizona.edu).

each dish. Confluent cultures were split to 2×10^6 cells/100 mm diameter dish and cultured for 20–24 h before treatment with H_2O_2. Cells were incubated with H_2O_2 at 37 °C and 5 % CO_2 in the culture medium for 2 h After removing H_2O_2 by changing the medium, the cells were incubated in fresh culture medium for an additional 2 h to 1 week, before harvesting for various measurements.

Trypan Blue staining for plasma-membrane integrity

The Trypan Blue solution (0.4 %; Gibco BRL) was diluted with an equal volume of PBS. Adherent cells were stained with 0.2 % Trypan Blue solution directly. The detached cells in the supernatant were spun down at 3300 ***g*** and were resuspended in 0.2 % Trypan Blue solution. The number of blue cells was scored under a phase-contrast optical microscope.

Caspase-3 activity assay

The detached cells were collected by centrifugation and were mixed with attached cells from the same dish (100 mm diameter), unless otherwise indicated. The combined cells were dissolved in 300 μl of lysis buffer (0.5 % Nonidet P40/0.5 mM EDTA/150 mM NaCl/50 mM Tris, pH 7.5). Protein concentration in cell lysates was measured by the Bradford method according to the manufacturer's (Bio-Rad, Hercules, CA, U.S.A.) instructions. Cell lysates containing 10 or 26.6 μg of protein were incubated for 1 h at 37 °C with 40 μM of acetyl-Asp-Glu-Val-Asp-7-amino-4-methylcoumarin (Alexis Biochemicals, San Diego, CA, U.S.A.) in 200 μl of reaction buffer (10 mM Hepes/0.05 M NaCl/2.5 mM dithiothreitol, pH 7.5). The released 7-amino-4-methylcoumarin (AMC) was measured using a 96-well fluorescence plate reader with an excitation wavelength of 365 nm and an emission wavelength of 450 nm [24]. The data were obtained by comparing fluorescence levels with those of control samples to determine the level of caspase-3 activation.

Propidium iodide (PdmI) staining for scoring apoptotic cells

The detached cells in the supernatant were collected by centrifugation at 3300 ***g*** for 10 min and were pooled with the same group of cells detached by trypsin treatment. The cells were fixed in 25 % (v/v) ethanol containing 15 mM $MgCl_2$. After RNase digestion (0.1 μg of RNase A and 2 units of RNase T1/ml at 37 °C for 1 h), the cells were stained with 0.5 μg/ml PdmI for at least 30 min. The numbers of condensed nuclei versus normal nuclei were scored under a fluorescence microscope.

Double staining for DNA-synthesis-competent cells and senescence-associated β-galactosidase (SA β-gal)-positive cells

Cells were treated with H_2O_2 for 2 h and allowed to recover for 5 days in DMEM, containing 10 % FBS. The cells were incubated in fresh medium containing 10 μM bromodeoxyuridine (BrdU) for 48 h before fixation for 5 min in PBS containing 2 % (v/v) formaldehyde. After three washes with PBS, the cells were incubated with staining solution [1 mg/ml 5-bromo-4-chloroindol-3-yl β-D-galactopyranoside ('X-Gal')/40 mM citric acid-sodium phosphate (pH 6.0)/5 mM potassium ferrocyanide/150 mM NaCl/2 mM $MgCl_2$] at 37 °C for 24 h [25]. After β-gal staining, the cells were washed with 70 % ethanol and PBS. The cells were hydrolysed in 4 M HCl for 20 min before incubation with anti-BrdU antibody (Sigma) in PBS containing 2 % BSA. The incorporated anti-BrdU antibody was detected by an alkaline phosphatase-conjugated secondary antibody and a colorimetric reaction using the substrates 4-Nitroblue Tetrazolium Choride and 5-bromo-4-chloroindol-3-yl phosphate. The cells with BrdU or β-gal stain were recorded with Kodak Ektachome 64 Tungsten slide film under a phase-contrast optical microscope.

Flow-cytometric analysis for cell-cycle position

The detached cells in the supernatant, or adherent cells after trypsin treatment, were fixed with 25 % ethanol containing 15 mM $MgCl_2$. After RNase digestion (0.1 μg of RNase A and 2 units of RNase T1/ml at 37 °C for 1 h), the cells were stained with 50 μg/ml PdmI for at least 30 min before analysis with a flow cytometer (Becton–Dickinson FACSorter) using CELLQuest software. The instrument was set to collect 20000 events or for 10 min, whichever came first.

Western-blot analysis

Attached cells were collected by scraping them off into a lysis buffer, and the detached cells in the supernatant were collected by centrifugation before resuspension in the lysis buffer. For total cell lysate, cells were lysed in the Laemmli buffer [0.12 M Tris (pH 6.8)/2.4 % (w/v) SDS/50 % (v/v) glycerol/freshly added 1 μg/ml aprotinin/10 μg/ml leupeptin/10 mM PMSF]. For soluble cell lysates, cells were lysed in radioimmunoprecipitation buffer [1 × PBS/1 % Nonidet P40/0.5 % sodium deoxycholate/0.1 % SDS/freshly added protease inhibitors]. The soluble fraction was collected by centrifugation at 15000 ***g*** after incubation on ice for 60 min. An equal volume of SDS reducing buffer [0.5 % Tris/10 % glycerol/2 % SDS/5 % (v/v) 2-mercaptoethanol, pH 6.8] was added to cell lysates and samples were boiled for 10 min at 95–100 °C. Protein concentration was determined by the bicinchoninic acid ('BCA') method according to the manufacturer's (Pierce, Rockford, IL, U.S.A.) instructions after trichloroacetic acid precipitation. Bromophenol Blue (final concn. 0.01 %) was added to the samples before an equal amount of proteins was loaded in each lane for electrophoresis and blotting as described in [16]. The PVDF membrane was incubated with a primary antibody against p53 (Ab-6; Oncogene Science, Uniondale, NY, U.S.A.), p21 (PharMingen, San Diego, CA, U.S.A.), c-Myc (clone 9E10, Santa Cruz Biotechnology, Santa Cruz, CA, U.S.A.), bcl-2 (clone 100, Santa Cruz Biotechnology) or bax (P-19, Santa Cruz Biotechnology) for 2 h. The proteins were detected by enhanced chemiluminescence as described in [16] and were quantified by an Eagle Eye II Image System with installed density-analysis software (Stratagene, La Jolla, CA, U.S.A.).

Infection with recombinant human papilloma virus (HPV) E6 or E7 retroviral constructs

The HPV type 16 E6 and E7 retrovirus producing cells were obtained from the American Type Culture Collection (Rockville, MD, U.S.A.) [26]. Exponentially growing IMR-90 cells were infected with retroviruses carrying either the HPV E6 or E7 gene and were selected for by 500 μg/ml G418 (BioWhittaker, Walkersville, MD, U.S.A.) as previously described in [16].

RESULTS

Dose response of H_2O_2 cytotoxicity and induction of apoptosis

Exponentially growing early-passage IMR-90 cells (PDL < 30) seeded at a density of 2×10^6/100 mm diameter dish were treated for 2 h with H_2O_2 at various concentrations from 50–350 μM. Since H_2O_2 can oxidize serum and growth factors in the medium, the cells were placed in fresh medium after H_2O_2 treatment to

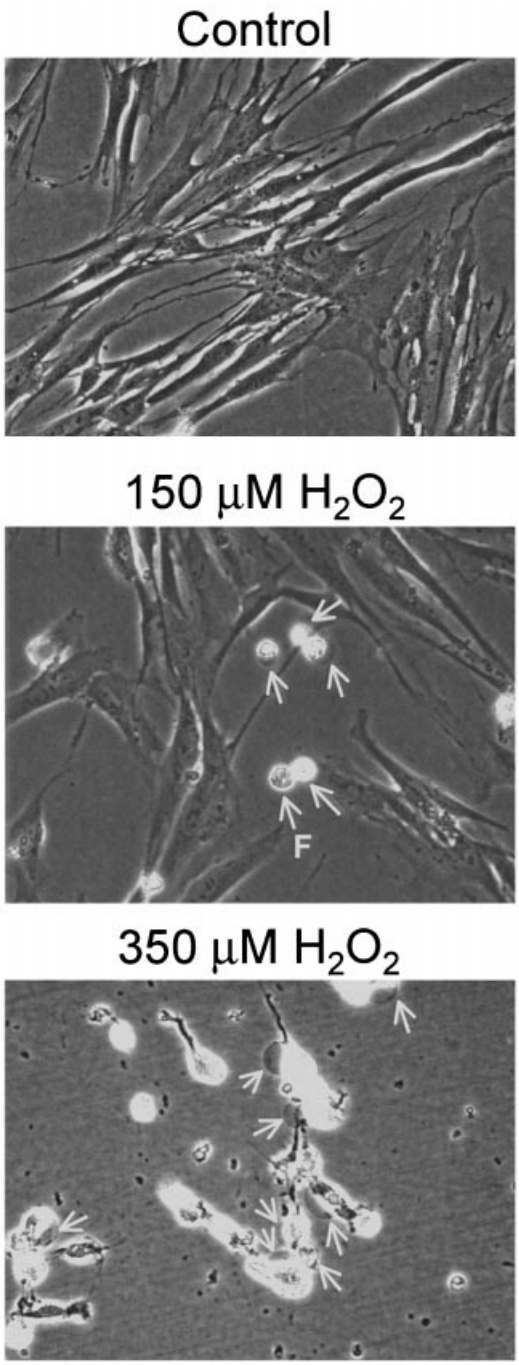

Figure 1 Morphology of IMR-90 cells after H_2O_2 treatment

Subconfluent cultures of IMR-90 cells (2×10^6 cells/100 mm diameter dish) were treated with 150 or 350 μM H_2O_2 for 2 h. At 24 h after removing H_2O_2, the morphology of untreated control cells (**A**), cells treated with 150 μM H_2O_2 (**B**) or cells treated with 350 μM H_2O_2 (**C**) was recorded by a digital camera attached to a phase-contrast microscope with 10 × lens using IPlab spectrum software. The arrows indicate detached and floating cells (**B**) or blebs in attached cells (**C**). F indicates the microscopic focusing point (**B**).

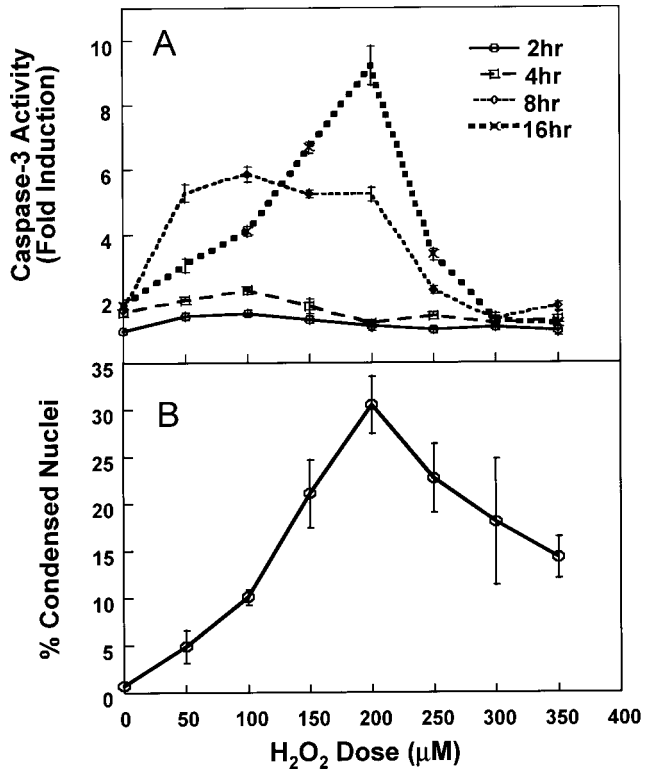

Figure 2 Dose-dependent activation of caspase-3 and induction of nuclear condensation

Subconfluent cultures of IMR-90 cells (2×10^6 cells/100 mm diameter dish) were treated for 2 h with various doses of H_2O_2. At 2, 4, 8 and 16 h after removing H_2O_2, the cells were harvested for measuring caspase-3 activity as described in the Materials and methods section (**A**). Condensed nuclei were quantified at 24 h after removing H_2O_2 (**B**).

eliminate the complication of nutrient deprivation. H_2O_2 at this concentration range did not appear to kill the cells immediately. The majority of cells treated with H_2O_2 at 150 μM or below remained attached and capable of excluding Trypan Blue (Figure 1). A small fraction of the cells rounded up, detached and floated into the medium in a time-dependent manner with 150 μM H_2O_2 (Figure 1) (see below). With 200, 250, 300 and 350 μM H_2O_2, the percentages of attached cells exhibiting Trypan Blue uptake were 5.0 ± 4.0, 26.7 ± 4.7, 38.3 ± 6.2 and $68.3 \pm 8.5\%$ at 4 h after removing H_2O_2 and were 33.3 ± 12.5, 70.0 ± 8.2, 100 ± 0 and 100 ± 0 (mean $\pm$ S.D., $n = 3$) at 16 h after removing H_2O_2. Dying cells resulting from high-concentration-H_2O_2 treatment remained attached before degradation, showed extensive membrane blebs and were distinct morphologically from detached cells resulting from treatment with H_2O_2 at 150 μM or lower (Figure 1). The killing dose varies with the density of cells and the presence of serum and is dependent on the concentration expressed as pmol/cell rather than the absolute concentration in μM. With the density of the culture and the protocol that we were using, H_2O_2 above 200 μM (or 1 pmol/cell) appeared to be cytotoxic. The cells appeared all dead 16 h after the treatment with 300 or 350 μM H_2O_2.

Activation of caspases is a hallmark of apoptosis in most biological systems. We measured caspase-3 activity at 2, 4, 8 and 16 h after treating cells with 50–350 μM H_2O_2. No activation of caspase-3 was observed at 2 or 4 h after H_2O_2 treatment with any of the doses (Figure 2A). At 8 h 50–200 μM H_2O_2-treated cells showed 5–6-fold induction of caspase-3 activity (Figure 2A). At 16 h caspase-3 activity showed a dose-dependent activation and reached a peak at 10-fold with 200 μM H_2O_2 (Figure 2A). H_2O_2 at 300 and 350 μM could not activate caspase-3 at any of the time points measured (Figure 2A).

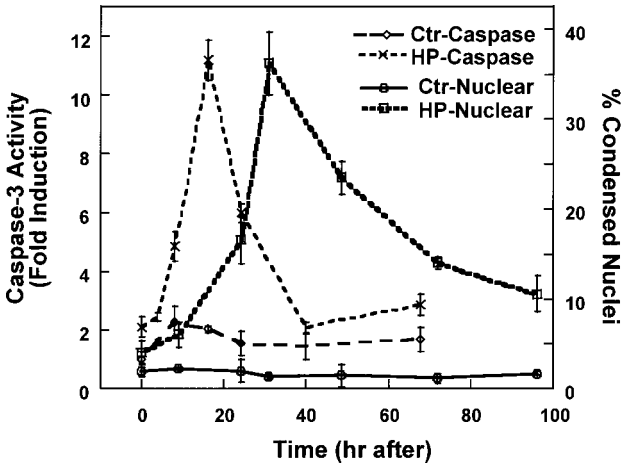

Figure 3 Time course of caspase-3 activation and nuclear condensation

Subconfluent cultures of IMR-90 cells (2×10^6 cells/100 mm diameter dish) were treated with 150 μM H_2O_2 for 2 h. At the indicated time, after removing H_2O_2, the cells were harvested for assaying caspase-3 activity or for scoring condensed nuclei as described in the Materials and methods section. Ctr, control; HP, H_2O_2.

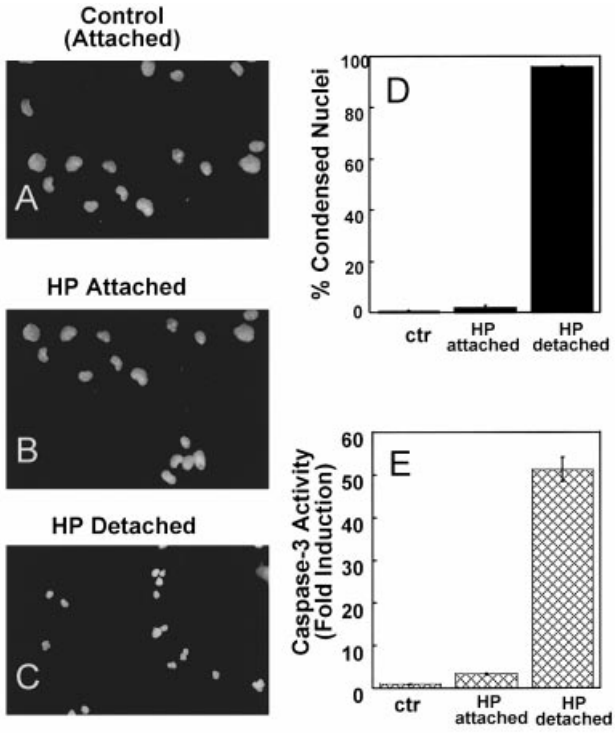

Figure 4 Nuclear morphology and caspase-3 activity in detached cells

Subconfluent cultures of IMR-90 cells (2×10^6 cells/100 mm diameter dish) were treated with 150 μM H_2O_2. At 24 h after removing H_2O_2, attached cells (**A**, **B** and **D**) were harvested by trypsin treatment and detached cells (**C** and **D**) were harvested by centrifugation for PdmI staining. Caspase-3 activity was determined at 20 h after removing H_2O_2 (**E**). HP, H_2O_2; ctr, control.

We examined nuclear morphology to test further that H_2O_2 at 200 μM or lower induced apoptosis. Condensed and shrunken nuclei were distinguishable from normal nuclei under the

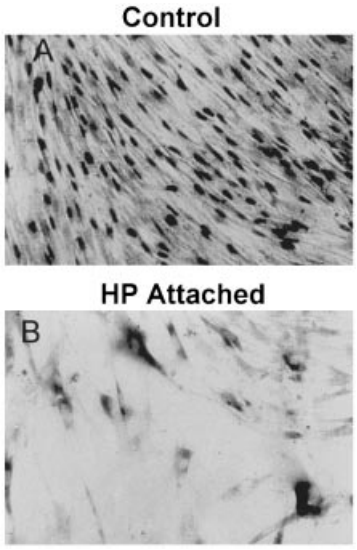

Figure 5 Loss of DNA synthesis and gain of SA β-gal activity in attached cells

At day 5 after 150 μM H_2O_2 treatment, untreated (**A**) or H_2O_2-treated cells (**B**) were labelled with 10 μM BrdU for 48 h before fixation for staining of BrdU-positive cells and SA β-gal-positive cells within same samples as described in the Materials and Methods section. The BrdU-positive stain is located in the nuclei, while the SA β-gal-positive stain shows increased intensity in the cytoplasm.

fluorescence microscope following low concentration PdmI staining. The results showed that H_2O_2 induced a dose-dependent increase in the proportion of condensed nuclei at 200 μM or lower (Figure 2B).

Using H_2O_2 at 150 μM (or 0.75 pmol/cell), we further characterized changes associated with apoptosis. Caspase-3 activity was first elevated at 8 h, reached a peak at 16 h and declined 24 h after H_2O_2 treatment (Figure 3). The percentage of condensed nuclei reached a plateau of 37% at 27 h and declined afterwards (Figure 3). Activation of caspase-3 preceded nuclear condensation.

Cell detachment is an early sign of apoptosis in many experimental systems. We observed that a fraction of cells rounded up, detached, and floated in the medium in a time-dependent manner. One representative experiment showed that 4.9 ± 2.4, 15.6 ± 2.8, 27.8 ± 2.7, 32.3 ± 5.7 and 30.3 ± 3.7% (means $\pm$ S.D. for three samples) cells detached after 150 μM H_2O_2 treatment at 8, 16, 24, 32 and 48 h respectively. Attached cells showed nuclear morphology indistinguishable from that of untreated (control) cells (Figures 4A and 4B). In contrast, nearly all detached cells contained condensed nuclei (Figures 4C and 4D). Measurement of caspase-3 activity at 20 h after H_2O_2 treatment revealed that detached cells contained most caspase-3 activity (Figure 4E). While pooled samples showed a maximal 10–11-fold induction of caspase-3 activity (Figures 2 and 3), detached cells showed an average 51-fold elevation of caspase-3 (Figure 4E). The majority of the detached cells were capable of excluding Trypan Blue until 21 h after H_2O_2 treatment. From 21–27 h there was a time-dependent increase in the proportion of detached cells taking up Trypan Blue. After 27 h most of the cells in the supernatant showed plasma-membrane leakage. The detached cells were collected at 24–27 h after 150 μM H_2O_2 treatment to assay for DNA ladder formation using agarose-gel electrophoresis after extracting DNA by two different methods

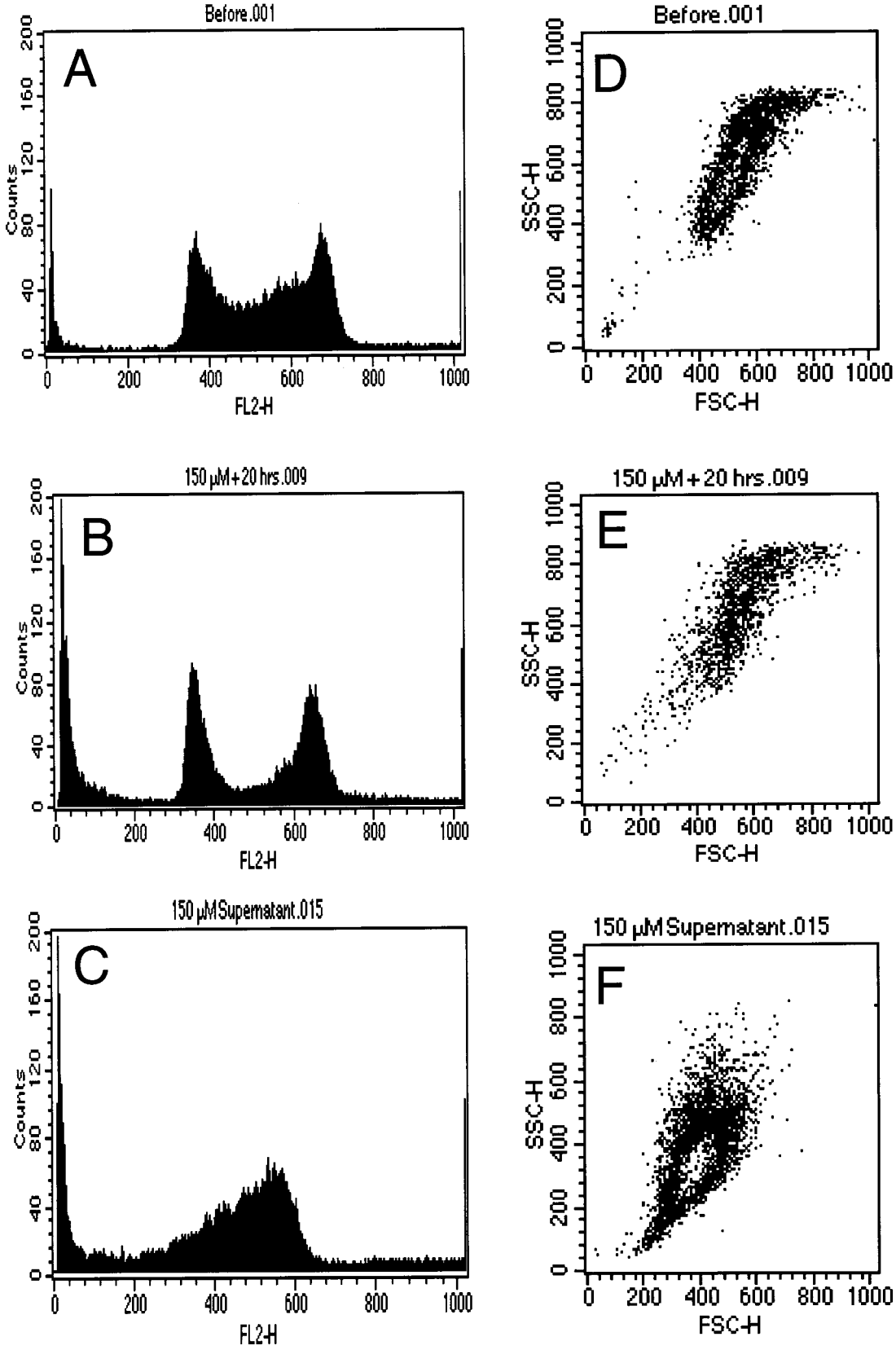

Figure 6 Cell-cycle distribution of apoptotic cells

Subconfluent cells (2×10^6 cells/100 mm diameter dish) (**A** and **D**) were treated with 150 μM H_2O_2 for 2 h. At 24 h after removing H_2O_2, cells remaining attached (growth-arrested cells) were collected by trypsin treatment (**B** and **E**) and cells in supernatant (apoptotic cells) were collected by centrifugation (**C** and **F**) for flow cytometric analysis.

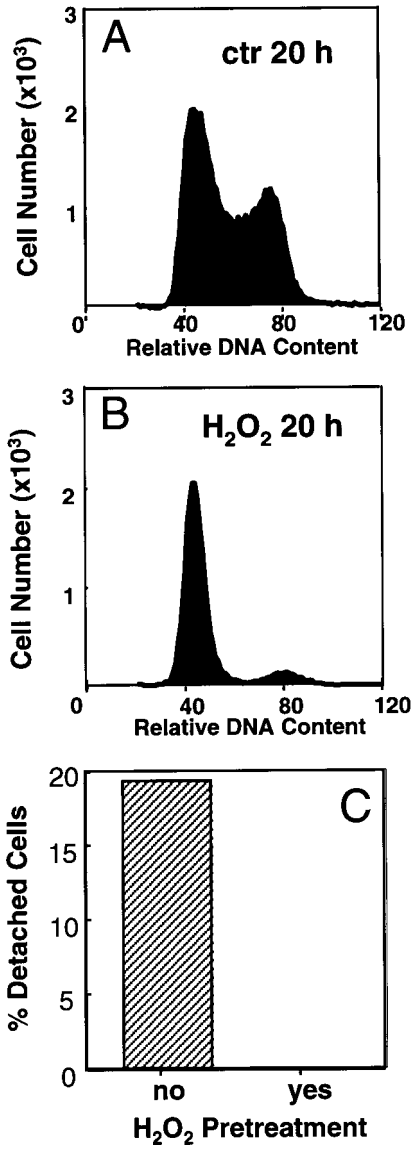

Figure 7 Induction of G1 arrest and inhibition of apoptosis

Confluent IMR-90 cells (6.5×10^6 cells/100 mm diameter dish) were treated with 550 μM H_2O_2 for 2 h. After treatment, the cells were split into new 100 mm diameter dishes at a density of 2×10^6 cells/dish. After cultivating for 20 h, untreated cells (**A**) or H_2O_2-pretreated cells (**B**) were harvested for cell-cycle analysis. The untreated cells or H_2O_2-pretreated cells were treated with 150 μM H_2O_2 for 2 h. At 24 h after the second H_2O_2 treatment, the percentage of apoptotic cells was determined by counting the number of attached cells and was calculated on the basis of cell loss by comparing the cell number with that before the second H_2O_2 treatment (**C**).

[27,28]. We did not observe a DNA ladder or smear in these cells (although a DNA ladder and smear were observed in serum-starved HeLa cells using the same protocols) (results not shown). Since H_2O_2 can cause DNA strand breaks in the absence of apoptosis, the terminal deoxynucleotidyl transferase-mediated dUTP–biotin nick-end labelling ('TUNEL') method cannot be used here to quantify apoptotic cells. Apoptosis was therefore judged by caspase-3 activation and morphological changes, including cell rounding up, cell detachment and nuclear condensation.

A large proportion of cells remained attached and capable of excluding Trypan Blue after treatment with 150 μM H_2O_2. These cells were growth-arrested, since they could not synthesize DNA when stimulated with serum or growth factors [14,15]. When these cells were kept under culture conditions for 1 week, approx. 94.6 ± 0.6 % of cells remained unable to synthesize DNA (Figure 5B). In comparison only 11.8 ± 5.3 % of untreated (control) cells were not able to synthesize DNA during the time frame (48 h) of BrdU labelling (Figure 5A). In addition, a large fraction of H_2O_2-treated cells appeared to resemble senescent cells morphologically (Figure 5B). The majority of H_2O_2-treated cells expressed senescent marker SA β-gal 7 days after H_2O_2 treatment. In brief, 150 μM H_2O_2 treatment results in two fractions: growth-arrested cells and apoptotic cells.

Cell-cycle distribution of apoptotic cells

Since the cells *en route* to apoptosis detached but remained intact until 27 h after H_2O_2 treatment, we could separate these cells from the rest of the growth-arrested cells. We used IMR-90 cells with a mixed-cell-cycle distribution in the G1, S and G2/M phases for H_2O_2 treatment (Figure 6A). At 24 h after H_2O_2 treatment, the attached cells showed a predominantly G1- or G2/M-phase distribution and a minimal S-phase distribution (Figure 6B). In contrast, the detached cells were mainly distributed in the S-phase (Figure 6C). The light-scattering data indicated the shrinkage of the detached cells (Figure 6F), when the data are compared to that of untreated (control) cells (Figure 6D) and H_2O_2-treated cells remaining attached (Figure 6E). These data suggest that the cells distributed in the S-phase of the cell cycle probably undergo apoptosis in response to treatment with 150 μM H_2O_2.

We examined the relationship between growth arrest and apoptosis. We found that quiescent cells and near-senescent cells, both of which are arrested in the G1 phase of the cell cycle, were reluctant to undergo apoptosis in response to H_2O_2. Quiescent cells were treated with sublethal 550 μM H_2O_2 (there were approx. 6.5×10^6 cells in each dish and the dose was equivalent to 0.85 pmol/cell). Upon subculture, untreated cells showed a mixed distribution in the G1, S and G2/M phases of the cell cycle (Figure 7A), while H_2O_2-pretreated cells showed only G1 distribution (Figure 7B). When the G1-arrested cells were subsequently treated with 150 μM H_2O_2 (or 0.75 pmol/cell), we did not observe any apoptotic cells at 24 h after the treatment (Figure 7C). This result suggests that pretreatment with H_2O_2 can induce G1 arrest and can also prevent apoptosis by subsequent H_2O_2 treatment.

Molecular changes in apoptotic cells

We collected growth-arrested and apoptotic cells separately and measured the levels of c-Myc, p53, p21, bcl-2 and bax in each fraction. Elevation of c-Myc has been implicated in the mechanism of chemically induced apoptosis [28,29]. Since apoptosis of IMR-90 cells is associated with S-phase distribution (Figure 6C), and c-Myc is elevated when cells progress from G1 to S phase, we tested whether H_2O_2 treatment caused an elevation of c-Myc protein. We did not observe an increase in c-Myc protein immediately or at 20 h after H_2O_2 treatment in growth-arrested or apoptotic cells (results not shown).

The p53 protein is elevated within 2 h of H_2O_2 treatment (Figure 8A). The data from five independent experiments, with samples collected at 20–24 h after H_2O_2 treatment, revealed that growth-arrested cells or apoptotic cells showed an average 3.5- or 6.1-fold elevation respectively of p53 (Figure 8A). Statistical comparison indicated that the difference in the fold induction of p53 between growth-arrested versus apoptotic cells was significant ($P < 0.01$ using Student's t test). Therefore p53 is elevated

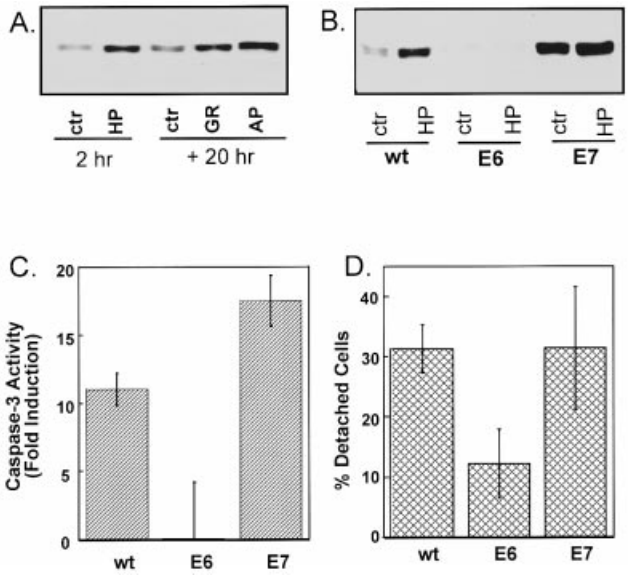

Figure 8 Role of p53 in H_2O_2-induced apoptosis

Subconfluent cultures of IMR-90 cells (2×10^6 cells/100 mm diameter dish) were treated with 150 μM H_2O_2 (HP) for 2 h. The cells were collected immediately (**A** and **B**) or were incubated in fresh medium for 20 h after removing H_2O_2 (**A**). Growth-arrested cells (GR) and apoptotic cells (AP) were collected separately for determination of p53 level by Western-blot analysis (**A**, 15 μg of protein/lane; **B,** 10 μg of protein/lane). Caspase-3 activity was measured at 16 h after the treatment (**C**). The percentage of apoptotic cells at 20 h after H_2O_2 treatment (**D**) was determined as described in Figure 7. wt, wild-type.

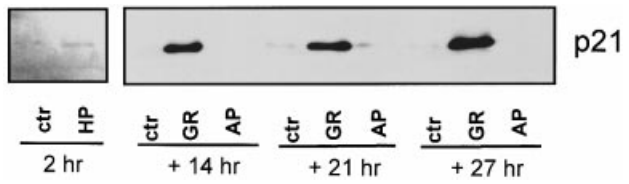

Figure 9 Absence of p21 in apoptotic cells

Subconfluent cultures of IMR-90 cells (2×10^6 cells/100 mm diameter dish) were treated with 150 μM H_2O_2 (HP) for 2 h and harvested immediately. At 14, 21 or 27 h after removing H_2O_2, growth arrested (GR) and apoptotic cells (AP) were harvested separately. The level of p21 protein was determined by gel electrophoresis (20 μg of protein/lane) and Western-blot analysis.

to a greater degree in apoptotic cells than in growth-arrested cells.

The role of p53 protein in H_2O_2-induced apoptosis was tested using HPV E6 protein [30,31]. The E6 protein reduced the basal level of p53 and prevented the induction of p53 by H_2O_2 in IMR-90 cells (Figure 8B). HPV E7 disrupts retinoblastoma function without affecting the level of p53 protein and serves as a comparison for HPV E6 (Figure 8B). Introducing HPV E6 or E7 into IMR-90 cells does not result in changes in cell morphology or in the dose response to H_2O_2 cytotoxicity. When IMR-90 cells carrying E6 were treated with H_2O_2, caspase-3 was not activated within 16 h and the fraction of apoptotic cells was reduced within 24 h (Figures 8C and 8D). In comparison, HPV E7 protein failed to reduce caspase-3 activity or the proportion of apoptotic cells (Figures 8B, 8C and 8D). The data indicate that H_2O_2-induced apoptosis of HDFs is probably p53-dependent.

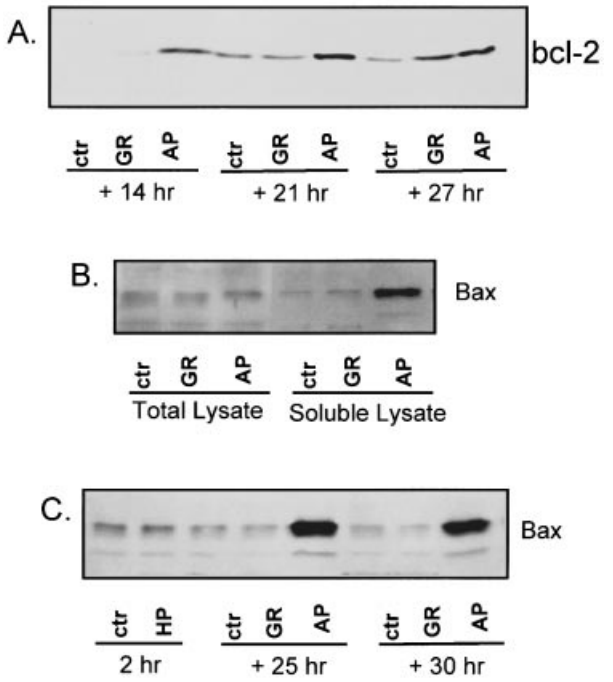

Figure 10 Levels of bcl-2 and bax proteins in growth-arrested or apoptotic cells

Subconfluent cultures of IMR-90 cells (2×10^6 cells/100 mm diameter dish) were treated with 150 μM H_2O_2 for 2 h and were harvested at 14, 21, or 27 h after the treatment. Growth-arrested (GR) and apoptotic cells (AP) were collected separately. The level of bcl-2 protein was determined by gel electrophoresis (20 μg protein/lane) and Western-blot analysis (**A**). The level of bax protein was determined in total cell lysate (**B**) or soluble cell lysate (**B** and **C**) by gel electrophoresis (5 μg of protein/lane) and Western-blot analysis.

The level of p21 protein was determined in growth-arrested and apoptotic cells. At 14–27 h after H_2O_2 treatment, the growth-arrested cells showed a dramatic elevation of p21 protein. In contrast, no elevation of p21 was observed in apoptotic cells (Figure 9).

The levels of bcl-2 and bax proteins were measured by Western-blot. We observed an elevation of bcl-2 protein at 14 h after H_2O_2 treatment and the elevation was sustained to 27 h in apoptotic cells (Figure 10A). Elevation of bcl-2 was also observed in growth-arrested cells at 27 h after H_2O_2 treatment (Figure 10A). The bax protein was first measured using total-cell lysates and we did not observe an elevation of bax protein in apoptotic cells (Figure 10B). Interestingly, when soluble cell extracts were prepared, we observed an increase of bax protein in apoptotic cells (Figure 10B). This soluble form of bax remained elevated in the apoptotic cells at later time points (30 h) when the plasma membrane became leaky (Figure 10C). Our data show no decrease in bcl-2 protein, but an increase in the solubility of the bax protein in apoptotic HDFs.

DISCUSSION

A fraction of exponentially growing IMR-90 cells underwent apoptosis in response to 50–200 μM H_2O_2. With a 2 h pulse treatment, H_2O_2 at this concentration range caused dose-dependent increases in caspase-3 activity and nuclear condensation. While apoptotic cells detached within 32 h after H_2O_2 treatment, the cells remaining attached were growth arrested and could develop features of senescence over 1 week. H_2O_2 above 300 μM

killed all the cells without caspase-3 activation. The time course and morphological changes of cell death induced by high doses differ from those induced by H_2O_2 at 150 μM or lower, suggesting that high-dose H_2O_2 probably causes necrosis instead of apoptosis.

Flow-cytometric analysis indicated that apoptotic cells were mainly distributed in the S-phase of the cell-cycle while the majority of growth-arrested cells were distributed in the G1 and G2/M phases of the cell cycle. A possible explanation of the observed S-phase distribution of apoptotic cells is that the cells in G2/M phase may undergo DNA degradation and register at S-phase during apoptosis. Since the DNA ladder or smear was not observed in the apoptotic cells during the time frame of the present study, it is unlikely that DNA degradation occurred in the early stage when the cell cycle distribution was analysed. The cells distributed in the G1 phase of the cell cycle remained G1-arrested [16] and serve as a reference for judging changes in the proportion of G2/M-phase cells. The area of the G2/M peak did not appear to be decreased compared with that of the G1 peak in the fraction that survived H_2O_2 treatment (Figure 6B). These observations do not support the argument that cells in the G2/M phase undergo apoptosis and register as S-phase cells.

An important caveat of inhibiting apoptosis with H_2O_2 pretreatment is induction of tolerance. A pretreatment with low-dose oxidants induces marked adaptive increases in H_2O_2 resistance in a number of cell lines [32,33]. Oxidants have been shown to induce the expression of superoxide dismutases and catalase in mammalian cells [34–36]. In addition, oxidants are known to induce the expression of heat-shock proteins [37]. These stress responses have been linked to increased tolerance to subsequent insults and resistance to apoptosis [38,39]. Therefore although pretreating quiescent cells with H_2O_2 can induce G1 arrest, such treatment can also induce tolerance.

Our data support the dual roles of p53 in growth arrest and apoptosis. Apoptotic cells showed a greater degree of p53 elevation than growth-arrested cells. Although the mechanism underlying the difference in the magnitude of p53 elevation and the functional impact of the difference are not understood, it is known that the p53 protein is a transcriptional activator of the p21-cyclin-dependent-kinase-inhibitor gene. In our experimental model, HPV E6 can reduce p53 and prevent induction of p21 in growth-arrested cells [16], indicating p53-dependency of p21 elevation. However, apoptotic cells showed an elevation of p53 protein, but an absence of the p21 protein (Figure 9). Recent studies indicated that p21 protein is a substrate of caspase-3 and can be cleaved at an early stage of apoptosis [40,41]. The activation of caspase-3 was detectable at 8 h while p21 was first measured at 14 h after H_2O_2 treatment. Therefore it is possible that p21 has been cleaved by caspase-3 in apoptotic HDFs. Nevertheless, it has been reported that the p21 protein is an antagonist of p53-dependent apoptosis. Induction of endogenous p21 or overexpression of p21 transgene prevents apoptosis [42,43]. The absence of p21 may be important for the cells to proceed with the rest of changes associated with apoptosis.

The bcl-2 protein is a survival factor, while bax is a death factor in a number of systems [20,21]. The bcl-2 protein resides on the mitochondrial membrane, endoplasmic reticulum and nuclear envelope. Bax normally localizes at nuclear and mitochondrial membranes [44]. The bax protein can form ion channels on mitochondrial membranes and induce the release of cytochrome *c* from mitochondria [45,46]. In contrast, bcl-2 is thought to form a dimer with bax and prevent the release of cytochrome *c* from mitochondria [46–49]. In agreement with Bladier et al. [50], we found that apoptotic cells had elevated bcl-2 protein after H_2O_2 treatment. This finding argues against the rule of bcl-2/bax ratio. However, increased solubility of bax may suggest its relocalization during apoptosis. Recently, Hsu and Youle [51] reported that bax is a soluble monomeric 25 kDa protein which does not form homodimers or heterodimers with other bcl-2 family members in apoptotic cells. *In vitro* experiments showed that bax could activate caspases in the cytosol in the presence of cytochrome *c* [45]. H_2O_2 has been shown to induce the mitochondrial membrane transition and release cytochrome *c* from mitochondria [52,53]. Taken together, our data and others suggest that bax, together with cytochrome *c* in the cytosol, causes activation of caspases.

Oxidants have been shown to mediate apoptosis induced by a variety of stimuli, including death receptor ligands and p53 inducers. Recent studies indicate that p53 controls apoptosis by activation of redox-responsive genes and generation of reactive oxygen species [54]. Given our results showing that oxidants can induce p53, there may exist a positive feedback loop that amplifies the p53 signal and oxidant production during the process of apoptosis. Nevertheless, death of normal somatic cells occurs as a consequence of aging, physical injury, ischaemic reperfusion, radiation and chemotherapy. Our study with HDFs may provide an understanding towards the mechanism of normal somatic cell death, which is important for designing therapies against unwanted cell death.

This work was supported by a Burroughs Wellcome New Investigator Award (to Q.M.C.), the start-up fund from the Department of Pharmacology, the Dean's Research Council Award from College of Medicine, University of Arizona (to Q.M.C.), and a National Institute of Environmental Health Training Grant (to J.B.M.).

REFERENCES

1 Ames, B. N., Shigenaga, M. K. and Hagen, T. M. (1993) Proc. Natl. Acad. Sci. U.S.A. **90**, 7915–7922
2 Halliwell, B. and Gutteridge, J. M. C. (1989) in Free Radicals in Biology and Medicine, pp. 416–508, Oxford University Press, Oxford
3 Kehrer, J. P. (1993) Crit. Rev. Toxicol. **23**, 21–48
4 Cadenas, E. (1989) Annu. Rev. Biochem. **58**, 79–110
5 Halliwell, B. and Gutteridge, J. M. C. (1989) in Free Radicals in Biology and Medicine, pp. 22–81, Oxford University Press, Oxford
6 Berlett, B. S. and Stadtman, E. R. (1997) J. Biol. Chem. **272**, 20313–20316
7 Campisi, J. (1996) Cell **84**, 497–500
8 Smith, J. R. and Pereira, S. O. (1996) Science **273**, 63–67
9 Goldstein, S. (1990) Science **249**, 1129–1133
10 Cristofalo, V. J. and Pignolo, R. J. (1993) Physiol. Rev. **73**, 617–638
11 Noda, A., Ning, Y., Venable, S. F., Pereira, S. O. and Smith, J. R. (1994) Exp. Cell Res. **211**, 90–98
12 Alcorta, D. A., Xiong, Y., Phelps, D., Hannon, G., Beach, D. and Barrett, J. C. (1996) Proc. Natl. Acad. Sci. U.S.A. **93**, 13742–13747
13 Campisi, J., Dimri, G. and Hara, E. (1996) in Handbook of the Biology of Aging (Schneider, E. and Rowe, J., eds.), pp. 121–149, Academic Press, New York
14 Chen, Q. and Ames, B. N. (1994) Proc. Natl. Acad. Sci. U.S.A. **91**, 4130–4134
15 Chen, Q. M. (2000) Ann. N. Y. Acad. Sci. U.S.A., in the press
16 Chen, Q. M., Bartholomew, J. C., Campisi, J., Acosta, M., Reagan, J. D. and Ames, B. N. (1998) Biochem. J. **332**, 43–50
17 Hale, A. J., Smith, C. A., Sutherland, L. C., Stoneman, V. E., Longthorne, V., Culhane, A. C. and Williams, G. T. (1996) Eur J. Biochem. **236**, 1–26
18 Vaux, D. L. and Strasser, A. (1996) Proc. Natl. Acad. Sci. U.S.A. **93**, 2239–2244
19 Evan, G. and Littlewood, T. (1998) Science **281**, 1317–1322
20 Reed, J. C. (1997) Nature (London) **387**, 773–776
21 Adams, J. M. and Cory, S. (1998) Science **281**, 1322–1326
22 Cohen, G. M. (1997) Biochem. J. **326**, 1–16
23 Thornberry, N. A. and Lazebnik, Y. (1998) Science **281**, 1312–1316
24 Mizushima, N., Koike, R., Kohsaka, H., Kushi, Y., Handa, S., Yagita, H. and Miyasaka, N. (1996) FEBS Lett. **395**, 267–271
25 Dimri, G., Lee, X., Basile, G., Acosta, M., Scott, G., Roskelley, C., Medrano, E., Linskens, M., Rubelj, I., Pereira-Smith, O. et al. (1995) Proc. Natl. Acad. Sci. U.S.A. **92**, 9363–9367

26 Halbert, C. L., Demers, G. W. and Galloway, D. A. (1991) J. Virol. **65**, 473–478
27 Shigenaga, M. K., Aboujaoude, E. N., Chen, Q. and Ames, B. N. (1994) Methods Enzymol. **234**, 16–33
28 Zhan, Y., Cleveland, J. L. and Stevens, J. L. (1997) Mol. Cell. Biol. **17**, 6755–6764
29 Thompson, E. B. (1998) Annu. Rev. Physiol. **60**, 575–600
30 Tommasino, M. and Crawford, L. (1995) Bioessays **17**, 509–518
31 Vousden, K. (1993) FASEB J. **7**, 872–879
32 Wiese, A. G., Pacifici, R. E. and Davies, K. J. (1995) Arch. Biochem. Biophy. **318**, 231–240
33 Crawford, D. R. and Davies, K. J. (1994) Environ. Health Perspect. **102**, 25–28
34 Janssen, Y. M., Van, H. B., Borm, P. J. and Mossman, B. T. (1993) Lab. Invest. **69**, 261–274
35 Yoo, H. Y., Chang, M. S. and Rho, H. M. (1999) J. Biol. Chem. **274**, 23887–23892
36 Lai, C. C., Peng, M., Huang, L., Huang, W. H. and Chiu, T. H. (1996) J. Mol. Cell. Cardiol. **28**, 1157–1163
37 Morimoto, R. I. (1993) Science **259**, 1409–1410
38 Samali, A. and Orrenius, S. (1998) Cell Stress Chaperones **3**, 228–236
39 Vayssier, M. and Polla, B. S. (1998) Cell Stress Chaperones **3**, 221–227
40 Zhang, Y., Fujita, N. and Tsuruo, T. (1999) Oncogene **18**, 1131–1138
41 Park, J. A., Kim, K. W., Kim, S. I. and Lee, S. K. (1998) Eur J. Biochem. **257**, 242–248
42 Bissonnette, N. and Hunting, D. J. (1998) Oncogene **16**, 3461–3469
43 Gorospe, M., Cirielli, C., Wang, X., Seth, P., Capogrossi, M. C. and Holbrook, N. J. (1997) Oncogene **14**, 929–935
44 Oltvai, Z. N., Milliman, C. L. and Korsmeyer, S. J. (1993) Cell **74**, 609–619
45 Jurgensmeier, J. M., Xie, Z., Deveraux, Q., Ellerby, L., Bredesen, D. and Reed, J. C. (1998) Proc. Natl. Acad. Sci. U.S.A. **95**, 4997–5002
46 Schlesinger, P. H., Gross, A., Yin, X. M., Yamamoto, K., Saito, M., Waksman, G. and Korsmeyer, S. J. (1997) Proc. Natl. Acad. Sci. U.S.A. **94**, 11357–11362
47 Antonsson, B., Conti, F., Ciavatta, A., Montessuit, S., Lewis, S., Martinou, I., Bernasconi, L., Bernard, A., Mermod, J. J., Mazzei, G. et al. (1997) Science **277**, 370–372
48 Yang, J., Liu, X., Bhalla, K., Kim, C. N., Ibrado, A. M., Cai, J., Peng, T. I., Jones, D. P. and Wang, X. (1997) Science **275**, 1129–1132
49 Kluck, R. M., Bossy-Wetzel, E., Green, D. R. and Newmeyer, D. D. (1997) Science **275**, 1132–1136
50 Bladier, C., Wolvetang, E. J., Hutchinson, P., de Haan, J. B. and Kola, I. (1997) Cell Growth Differ. **8**, 589–598
51 Hsu, Y. T. and Youle, R. J. (1998) J. Biol. Chem. **273**, 10777–10783
52 Takeyama, N., Matsuo, N. and Tanaka, T. (1993) Biochem. J. **294**, 719–725
53 Stridh, H., Kimland, M., Jones, D. P., Orrenius, S. and Hampton, M. B. (1998) FEBS Lett. **429**, 351–355
54 Polyak, K., Xia, Y., Zweier, J. L., Kinzler, K. W. and Vogelstein, B. (1997) Nature (London) **389**, 300–305

Received 22 June 1999/28 October 1999; accepted 15 February 2000